Enantiomeric Analysis of Planar Chiral (η^6-Arene)chromium Tricarbonyl Complexes using NMR in Oriented Solvents

Olivier Lafon and Philippe Lesot*

Laboratoire de Chimie Structurale Organique, ICMMO, UMR 8074, Bâtiment 410, Université de Paris-Sud, 91405 Orsay Cedex, France

Michaël Rivard, Murielle Chavarot,* Françoise Rose-Munch,* and Eric Rose

Laboratoire de Chimie Organique, UMR 7611, Tour 44/45, 1er étage, case 181, Université Pierre et Marie Curie, 75252 Paris Cedex 05, France

Received March 30, 2005

We investigate the analytical potential of proton-decoupled and proton-coupled carbon-13 NMR spectroscopy in chiral polypeptide liquid crystals for the enantiomeric discrimination of planar chiral (η^6-arene)chromium tricarbonyl complexes. Experimental results obtained for chiral β-hydroxyamino alcohol and a series of chiral aldehydic complexes are reported and discussed in detail.

Introduction

Planar chiral (η^6-arene)chromium tricarbonyl complexes are a versatile class of chiral auxiliaries which have found numerous applications in asymmetric synthesis[1] and have also recently emerged as original ligands for enantioselective catalysis.[2] Their success relies mainly on the following considerations: (i) both enantiomers of chiral complexes can be easily prepared, by resolution of a racemic mixture,[3] by diastereoselective complexation,[3,4] or by asymmetric synthesis;[5] (ii) the stereodirecting effects of the $Cr(CO)_3$ organometallic moiety[1b] induce high levels of diastereoselectivity for a large variety of reactions.

Recently, we described the first asymmetric SmI_2-induced cross-coupling of planar chiral $Cr(CO)_3$ aromatic nitrone complexes with carbonyl compounds.[6] This highly chemoselective reaction provides a new and direct access to β-*N*-hydroxylamino alcohols and β-amino alcohols with high yields (>80%) and excellent diastereoselectivities (dr > 95:5).

The enantiopure version of this coupling (Scheme 1) was developed by starting with the *o*-methylbenzaldehyde complex **(*pR*)-1**, which was prepared according to a procedure described a few years ago.[3] Its enantiomeric excess (ee), i.e. 98%, was determined by optical rotation measurement. The nitrone **(*pR*)-2** was then prepared by condensation of *N*-benzylhydroxylamine with **(*pR*)-1**. The complete diastereoselectivity of the reductive cross-coupling between **(*pR*)-2** and the acetone was determined from the ^{1}H NMR analysis of the crude mixture. Indeed, only one diastereoisomer was detected and isolated. In view of the importance of such β-amino alcohol derivatives in organic synthesis and catalysis,[7] we wished to confirm the enantiomeric purity of the complexes obtained by this new and useful synthetic procedure.

The enantiomeric purity of planar chiral (arene)-chromium derivatives has so far been determined by optical rotation measurements, chiral HPLC analysis,[8] and ^{1}H NMR using chiral derivatizing agents[3,5c] (CDA) or shift reagents.[9] Since the β-amino alcohol **(*pR,S*)-3** and β-*N*-hydroxylamino alcohol **(*pR,S*)-4** are being described for the first time, no reference was available for comparison with their $[\alpha]_D$ values. Although the HPLC analysis seems to be a rather general technique from a substrate point of view, it requires sometimes specific or expensive equipment, and finding optimal

* To whom correspondence should be addressed. E-mail: philesot@icmo.u-psud.fr (P.L.) (for NMR in oriented solvents); chavarot@ccr.jussieu.fr (M.C.); rosemun@ccr.jussieu.fr (F.R.-M.) (for chemistry of complexes).

(1) (a) Solladié-Cavallo, A. In *Advances in Metal-Organic Chemistry*; Liebeskind, L. S., Ed.; JAI: Greenwich, CT, 1989; Vol. 1, p 99. (b) Davies, S. G. and McCarthy, T. D. *Transition Metal Arene Complexes: Side-Chain Activation and Control of Stereochemistry* in *Comprehensive Organometallic Chemistry II*; Eds. Abel, E. W., Stone, F. G. A., Wilkinson, G., Eds.; Pergamon: Oxford, U.K., 1995; Vol. 12, p 1039.

(2) (a) Bolm, C.; Muñiz, K. *Chem. Soc. Rev*. **1999**, *28*, 51. (b) Gibson, S. E.; Ibrahim, H. *Chem. Commun*. **2002**, 2465. (c) Salser, A. *Coord. Chem. Rev*. **2003**, *242*, 59.

(3) Alexakis, A.; Mangeney, P.; Marek, I.; Rose-Munch, F.; Rose, E.; Semra, A.; Robert, F. *J. Am. Chem. Soc.* **1992**, *114*, 8288 and references therein.

(4) Tweddell, J.; Hoic, D. A. Fu, G. C. *J. Org. Chem.* **1997**, *62*, 8286.

(5) Selected references: (a) Rose-Munch, F.; Aniss, K.; Rose, E.; Vaissermann, J. *J. Organomet. Chem*. **1991**, *415*, 233. (b) Alexakis, A.; Kanger, T.; Mangeney, P.; Rose-Munch, F.; Perrotey, A.; Rose, E. *Tetrahedron: Asymmetry* **1995**, *6*, 47. (c) Alexakis, A.; Kanger, T.; Mangeney, P.; Rose-Munch, F.; Perrotey, A.; Rose, E. *Tetrahedron: Asymmetry* **1995**, *6*, 2135. (d) Gibson, S. E.; Reddington, E. G. *Chem. Commun*. **2000**, 989. (e) Overman, L. E.; Owen, C. E.; Zipp, G. G. *Angew. Chem., Int. Ed*. **2002**, *41*, 3884.

(6) Chavarot, M.; Rivard, M.; Rose-Munch, F.; Rose, E.; Py, S. *Chem. Commun*. **2004**, 2330.

(7) (a) Soai, K.; Niwa, S. *Chem. Rev.* **1992**, *92*, 833. (b) Ager, D. J.; Prakash, I.; Schaad, D. R. *Chem. Rev.* **1996**, *96*, 835. (c) Bergmeier, S. C. *Tetrahedron* **2000**, *56*, 2561. (d) Pu, L.; Yu, H.-B. *Chem. Rev.* **2001**, *101*, 757.

(8) (a) Villani, C.; Pirkle, W. H. *J. Chromatogr. A* **1995**, *693*, 63. (b) Bitterwolf, T. E.; Hubler, T. L. *J. Organomet. Chem*. **1995**, *487*, 119. (c) Pertici, P.; Borgherini, F.; Vitulli, G.; Salvadori, P.; Rosini, C.; Moïse, C.; Besançon, J. *Inorg. Chim. Acta* **1998**, *268*, 323.

(9) (a) Solladié-Cavallo, A.; Suffert, J. *J. Magn. Reson. Chem*. **1985**, *23*, 739. (b) Ratni, H.; Jodry, J. J.; Lacour, J.; Kündig, E. P. *Organometallics* **2000**, *19*, 3997.

10.1021/om050239u CCC: $30.25
Publication on Web 06/28/2005

Scheme 1. Preparation of the *β*-Amino Alcohol (*pR,S*)-3 and *β*-*N*-Hydroxylamino Alcohol (*pR,S*)-4 via an Asymmetric Cross-Coupling between the Chiral Nitrone (*pR*)-2 and Acetone

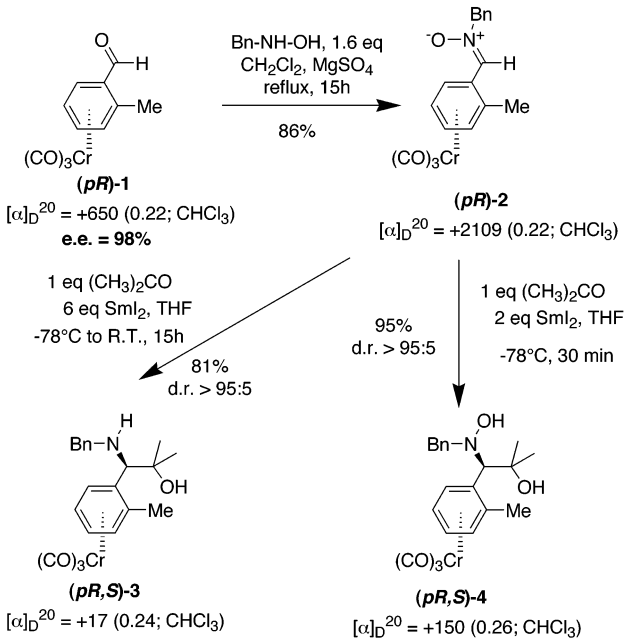

analytical conditions can be tedious. In contrast, isotropic NMR methods appear to be simpler but have been scarcely developed thus far. The first method[9a] takes advantage of a well-known chiral lanthanide shift reagent and has been successfully applied to various metal carbonyl complexes bearing an aldehyde group. The second method[9b] is an original application of the chiral TRISPHAT anion to neutral molecules, and its efficiency was specifically demonstrated for (arene)-chromium complexes substituted by either an aldehyde or a nitrone function.

In this context, it was pertinent to explore a new practical tool for the enantiomeric analysis of any type of planar chiral chromium complex. Hence, we turned our attention to NMR spectroscopy in the presence of chiral ordering agents (COA's) provided by weakly oriented polypeptidic chiral liquid crystals (CLC's).[10,11] This emerging technique offers two advantages compared with other NMR approaches. First neither specific chemical functionalities nor particular molecular geometries (rigid, flexible, with or without stereogenic center, ...)[12,13] for the analyte are required. Indeed the enantiodiscrimination is a consequence of the differential orientational ordering of two enantiomers interacting with a chiral oriented environment.[14] The second advantage is that NMR spectroscopy provides numerous versatile tools to differentiate between the signals of enantiomers. Historically this technique has been applied using chiral, isotopically enriched compounds.[15] Among the successful results, it was reported that enantiomers of chiral (η^4-1,3-diene)iron tricarbonyl complexes could be discriminated through proton-decoupled deuterium NMR.[16] Although this tool is highly useful, it requires the introduction of deuterium nuclei inside the chiral compounds. This synthetic step is not always trivial, and thus, it could appear to be a limitation for the technique. However, NMR using COA's is a very flexible approach because any magnetically active nuclei, such as proton, carbon-13, or fluorine-19 atoms, for instance, are potential NMR probes for our purposes.[11]

In this work, we have mainly exploited the potential of proton-decoupled carbon-13 NMR ($^{13}C\{^1H\}$ NMR)[17,18] using organic solutions of poly-γ-benzyl-L-glutamate (PBLG) to enantiodiscriminate the signal of chiral chromium tricarbonyl complexes. This paper will be presented as follows. In the first part, we will experimentally determine the ee value of the *β*-*N*-hydroxylamino alcohol **(*pR,S*)-4** prepared according to Scheme 1. Next, we will describe the ability of $^{13}C\{^1H\}$ NMR in CLC to discriminate between enantiomers of various chiral (η^6-arene)chromium tricarbonyl compounds. The results will be compared and discussed. An example of chiral discrimination based on the difference of $^{13}C-^1H$ heteronuclear dipolar couplings will also be presented.

Results and Discussion

Proton-Decoupled Carbon-13 1D NMR. When they are embedded in an oriented environment, solute molecules are partially ordered.[10] This molecular ordering can be described by a second-rank order tensor associated to a molecule fixed frame (abc), and denoted as the Saupe matrix, $\{\mathbf{S}_{\alpha\beta}\}$. This situation also arises when the solvent is a chiral liquid crystal. Nevertheless, in this case, the difference of interaction potential between solute enantiomers and the chiral mesophase generally produces differences in orientational ordering for *S* and *R* that can be measured using NMR spectroscopy.

In a chiral anisotropic solvent, the resonance frequency ν_C of any carbon-13 nucleus contains an isotropic (σ_C^{iso}) and an anisotropic ($\Delta\sigma_C^{S\text{ or }R}$) contribution to the electronic shielding. It can be written for *S* and *R* isomers as[10,18]

$$\nu_C^{S\text{ or }R} = \frac{\gamma}{2\pi}[1 - \sigma_C^{iso} - \Delta\sigma_C^{S\text{ or }R}]B_o \qquad (1)$$

where B_o is the strength of the magnetic field. Expressed in a molecular frame (*a*, *b*, *c*), the terms σ_C^{iso} and $\Delta\sigma_C^{S\text{ or }R}$ for each carbon atom are defined as

$$\sigma_C^{iso} = \frac{1}{3}(\sigma_{aa} + \sigma_{bb} + \sigma_{cc}) \qquad (2)$$

and

(10) Sarfati, M.; Lesot, P.; Merlet, D.; Courtieu, J. *Chem. Commun.* **2000**, 2069 and references therein.
(11) Aroulanda, C.; Sarfati, M.; Courtieu, J.; Lesot, P. *Enantiomer* **2001**, *6*, 281.
(12) Lesot, P.; Sarfati, M.; Courtieu, J. *Chem. Eur. J.* **2003**, *9,* 1794.
(13) Lesot, P.; Merlet, D.; Sarfati, M.; Courtieu, J.; Zimmermann, H.; Luz, Z. *J. Am. Chem. Soc.* **2002**, *124*, 10071.
(14) (a) Lesot, P.; Merlet, D.; Courtieu, J.; Rantala, R. R.; Jokisaari, J. *J. Phys. Chem.* **1997***, 101,* 571. (b) Emsley, J. W.; Lesot, P.; Merlet, D. *Phys. Chem. Chem. Phys.* **2004**, *6*, 522.
(15) Canet, I.; Courtieu, J.; Loewenstein, A.; Meddour, A. *J. Am. Chem. Soc.* **1995**, *117*, 6520.
(16) Canet, J.-L.; Canet, I., Gelas, J.; Ripoche, I.; Troin, Y. *Tetrahedron: Asymmetry* **1997**, *14*, 2447.
(17) Lesot, P.; Merlet, D.; Meddour, A.; Loewenstein, A.; Courtieu, J. *J. Chem. Soc., Faraday Trans.* **1995**, *91*, 1371.
(18) Meddour, A.; Berdagué, P.; Hedli, A.; Courtieu, J.; Lesot, P. *J. Am. Chem. Soc.* **1997**, *119*, 4502.

$$\Delta\sigma_C^{S \text{ or } R} = \frac{2}{3}\sum_{\alpha,\beta=a,b,c} \sigma_{\alpha\beta} S_{\alpha\beta}^{S \text{ or } R} \quad (3)$$

$\Delta\sigma_C^{S \text{ or } R}$ is referred to as the ^{13}C chemical shift anisotropy (^{13}C CSA) and depends on the Saupe matrix elements, $S_{\alpha\beta}^{S \text{ or } R}$, as shown in eq 3. Equation 1 indicates that chiral discrimination is detected in $^{13}C\{^1H\}$ NMR spectra when $\nu_C^S - \nu_C^R \neq 0$. As the term σ_C^{iso} is independent of the molecular ordering and is identical for enantiomers, chiral discrimination occurs when $\Delta\sigma_C^S$ significantly differs from $\Delta\sigma_C^R$. From a practical point of view, satisfactory spectral separations are obtained when chemical shift differences for *S* and *R* are larger than half of the line width of corresponding peaks.

From a theoretical point of view, all physical factors increasing either the difference in order parameters between enantiomers or the electronic shielding anisotropy of a carbon atom (electronic effect induced by the nature of substituents bonded or the hybridization state) will improve the ^{13}C CSA differences ($\Delta\Delta\sigma$). Thus, carbon atoms with an sp or sp^2 hybridization state generally provide better nuclear probes than sp^3 carbon atoms.[10,18]

In addition, the differences observed between spectra directly depend on the strength of B_o (see eq 1). In practice, when the enantiorecognition by the polymer occurs, the stronger the magnetic field, the larger the spectral separations, on the basis of CSA differences.

Spectral Analysis of Chiral Compound 4 and the Parent Derivatives 5 and 6. The assignment of ^{13}C signals for compounds **4**−**6** (Figure 1) in the isotropic phase was made on the basis of ^{13}C chemical shifts and was confirmed using heteronuclear proton/carbon-13 2D correlation experiments (HMQC) or using a spectral simulation program (ACD software). ^{13}C chemical shifts in $CDCl_3$ are given in the Experimental Section. Some comments can be made on these values. Due to the complexation of the $Cr(CO)_3$ moiety, the signals of chromium-complexed aromatic carbons (**4** and **5**) resonate rather downfield from those of classical benzene rings and are split over a larger chemical shift range. This situation originates from both electronic effects (i.e. magnetic anisotropy) and conformational effects of the $Cr(CO)_3$ tripod.[19] Thus, in **4** and **5**, the ^{13}C chemical shifts of the η^6-arene group range between 86 and 112 ppm, whereas those of the benzylic group vary between 127 and 138 ppm. Consequently, the assignment of the various peaks for each ring is strongly facilitated. In contrast, the assignment of aromatic carbon atoms for **6** is more complex but is still possible.

Finally, from a stereochemical point of view, we can note that methyl groups 9 and 10, in compounds **4**−**6**, are diastereotopic and so give rise to two distinct ^{13}C resonances regardless of the type of solvent (oriented or not, chiral or not). For the same reason, the aromatic carbon atoms (2/6) and (3/5) in compound **5** show two distinct ^{13}C resonances for each pair. In both situations, the absolute assignment of these diastereotopic elements is not trivial and was not performed.

(19) (a) Solladié-Cavallo, A.; Suffert, J. J. *Org. Magn. Reson.* **1980**, 14, 426. (b) Schleyer, P. v. R.; Kiran, B.; Simion, D. V., Sorensen, T. S. *J. Am. Chem. Soc.* **2000**, *122*, 510.

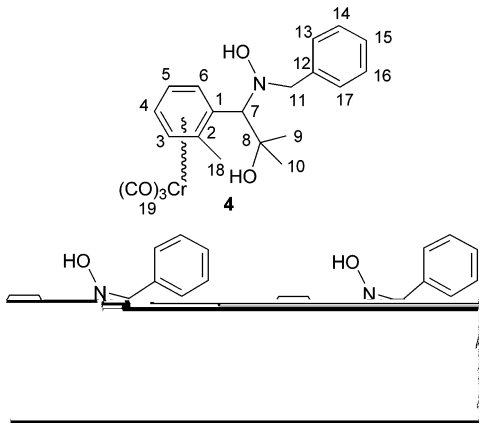

Figure 1. Molecular structure and chemical numbering of compounds **4**−**6** used in this work.

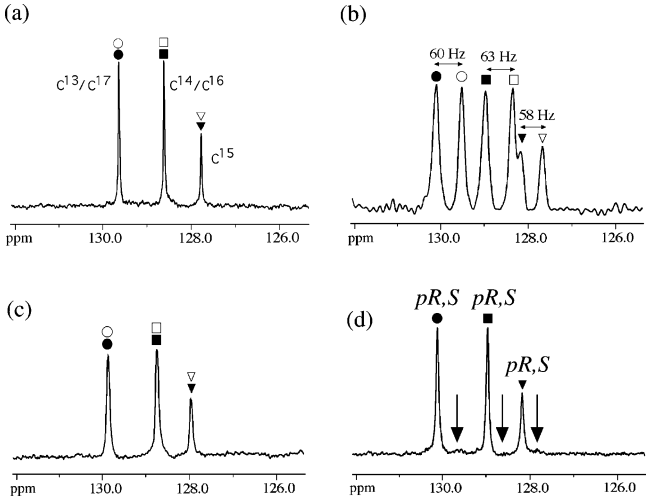

Figure 2. 100 MHz $^{13}C\{^1H\}$ NMR spectrum (aromatic region) of ***rac*-4** dissolved in (a) $CDCl_3$, (b) PBLG/chloroform, and (c) PBG/chloroform. (d) Same spectrum as (b) but using (***pR,S*)-4**. The $^{13}C\{^1H\}$ spectra in parts a−d were recorded by adding 2000, 6000, 5000, and 7000 scans, respectively. No filtering was used. Due to the proximity of broad resonances belonging to the aromatic signal of PBLG, a baseline correction was applied. All peaks marked with open symbols correspond to the (***pR,S*)-4** enantiomer.

In the field of chiral analysis, $^{13}C\{^1H\}$ NMR spectroscopy at the natural-abundance level is advantageous for various reasons. First, chiral discriminations can be observed on different carbon atoms of the molecule with no isotopic enrichment step. Second, the comparison between $^{13}C\{^1H\}$ spectra recorded in the liquid phase and the chiral mesophase generally indicates easily which carbon atoms are spectrally enantiodiscriminated. As an illustration, Figure 2a,b displays the $^{13}C\{^1H\}$ resonances of carbon atoms C^{13}/C^{17}, C^{14}/C^{16}, and C^{15} for the noncomplexed benzylic group of **(*rac*)-4** and (***pR,S*/*pS,R*)-4**, dissolved in $CDCl_3$ and the PBLG/chloroform phase, respectively. The doubling of these aromatic ^{13}C resonances observed in Figure 2b clearly indicate the ability of the chiral mesophase to differently orient the two enantiomers, thus producing separated signals, one for each enantiomer. Other carbon atoms of the molecule, including the carbonyl groups of the $Cr(CO)_3$ tripod and sp^3 carbon atoms are discriminated. All results are listed in Table 1.

Table 1. Differences of ^{13}C Chemical Shift (in Hz) for Chiral Compounds 4−6 in the PBLG/ Chloroform or PBLG/DMF Phase

		compound				
		4		**5**	**6**	
atom[a]	type of carbon	$CHCl_3$	DMF	$CHCl_3$	$CHCl_3$	DMF
1	C/sp^2	<lw[d]	0	41	[c]	0
2	C or CH/sp^2	93	9	22/35[e]	[c]	0
3	CH/sp^2	[c]	0	0/19[e]	[c]	7
4	CH/sp^2	42	10	40	0	0
5	CH/sp^2	0	0	19/0[e]	0	0
6	CH/sp^2	[c]	0	35/22[e]	[c]	<lw[d]
7	CH/sp^3	0	0	0	[c]	0
8	C/sp^3	0	0	<lw[d]	0	0
9[b]	CH_3/sp^3	0	0	0	13	0
10[b]	CH_3/sp^3	33	0	0	17	0
11	CH_2/sp^3	<lw[d]	<lw[d]	0	[c]	<lw[d]
12	C/sp^2	37	11	163	95	11
13/17	CH/sp^2	59	0	106	38	10
14/16	CH/sp^2	62	0	107	42	11
15	CH/sp^2	50	9	av[f]	89	12
18	CH_3/sp^3	28	0		[c]	0
19	C/sp	12	0	<lw[d]		

[a] The numbering is given in Figure 1. [b] Due to the diastereotopicity of methyl groups 9 and 10, the peak assignment might be inverted. [c] Abnormally large signal with very low signal to noise ratio (see text). [d] Limit of enantioseparations obtained when differences are below the line width of peaks. [e] Peak assignment might be inverted due to the diastereotopicity of carbon atoms 2/6 and carbon atoms 3/5. [f] Ambiguous value.

Due to a reduced molecular mobility in oriented phases, the T_2 transversal relaxation times are generally smaller than in isotropic phases, leading to a slight increase of the line widths. In case of compound **4**, we have observed an important deformation of ^{13}C peak (intensity and line width) for carbons C^3 and C^6 in the anisotropic phase compared to the corresponding signals in the isotropic phase. Such a situation can arise when the extreme narrowing conditions (for which molecular motions are rapid) are no longer satisfied[20] or if coalescence effects induced by a conformational exchange occur.[20] The reduction of the phenomenon at higher sample temperature suggests a possible coalescence effect due to a slow conformational exchange of the ligand around the C^1-C^7 bond. The presence of the methyl group in the η^6-arene moiety would favor this situation by hindering the rotation around the C^1-C^7 bond. This assumption can be supported by the fact that no effect was observed for ***rac*-5**. However, as we will discuss below, other phenomena related to transversal relaxation processes in PBLG phases could also contribute to the increase of line widths observed for some C-13 peaks.

To confirm the origin of ^{13}C signal doubling in these aromatic carbons, we have recorded ***rac*-4** in the achiral mesophase made of a racemic mixture of PBLG and PBDG, its enantiomer. In such a mixture, denoted "PBG", enantiomers are diffusing very rapidly, on the NMR time scale, from the vicinity of PBLG and PBDG helices, resulting in identical average magnetic interactions for each isomer and thereby eliminating chiral discrimination.[21] As expected, we observe the collapsing of aromatic $^{13}C\{^1H\}$ signals in Figure 2c, thus showing the cancellation of the chiral discrimination. Except for the shift due to ^{13}C CSA and solvent effects, the spectrum is formally identical with that recorded in liquid solvents. Note, however, that the deformation of the ^{13}C peak for C^3 and C^6 is also observed in the PBG phase and seems to confirm again a possible coalescence effect due to a conformational exchange of the *β-N*-hydroxylamino alcohol ligand.

Finally, Figure 2d reports the $^{13}C\{^1H\}$ signals of C^{13}/C^{17}, C^{14}/C^{16}, and C^{15} carbon atoms of the *β-N*-hydroxylamino alcohol (***pR,S*)-4** prepared according to Scheme 1. The absence of clearly emerging peaks for the minor enantiomer, (***pS,R*)-4**, indicates that the ee is over 95%. Such a result validates unambiguously the ee conservation all along the synthesis. Consequently NMR results in CLC permit us to definitely confirm the measurements of the optical rotation reported previously.[7]

The comparison of resonances with the spectrum in Figure 2b allows the ***pR,S*/*pS,R*** assignment for each ^{13}C peak. In Figure 2b, we can see that the most deshielded ^{13}C signals correspond to the **(*pR,S*)-4** enantiomer. This situation is nevertheless fortuitous, because there is no simple relationship between the absolute configuration of enantiomers and the relative positions of resonances observed for a given carbon atom. Thus, for instance, the most shielded signal for the C^2 and C^4 carbon atom in the η^6-arene group corresponds to the **(*pS,R*)-4** enantiomer.

In this molecule, a very small discrimination is observed for the carbonyl group (C^{19}) of the tripod. This can be rather surprising, considering the hybridization state of these carbon atoms (sp), for which a generally large spectral separation can be expected. Actually, the free rotation of the $Cr(CO)_3$ tripod under the arene ring (fast on the NMR time scale) averages the parameters that can be at the origin of the chiral discrimination (if the tripod was fixed), thus leading to small spectral enantioseparations. In contrast, the ^{13}C CSA differences are particularly large for some carbons. In particular, the values obtained for the benzylic ring (59−62 Hz) are rather intriguing.

For a better understanding of the origin of chiral discriminations for **4** and the large differences of ^{13}C CSA, we have investigated two parent derivatives (**5** and **6**) in the racemic series. As seen in Figure 1, both compounds are chiral, but planar chirality no longer exists, and hence this molecular property could not account for the enantiodiscriminations observed. To compare the results, ^{13}C NMR spectra of **4**−**6** were recorded using the same experimental conditions.

In Table 1 are listed the differences of ^{13}C CSA measured for compounds **5** and **6** in PBLG/chloroform. Both compounds still show spectral enantiodiscriminations on numerous ^{13}C sites and with various magnitudes, thus evidencing the ability of polypeptide to orient differently the enantiomers for the chiral organometallic complex **5** and the purely organic derivative **6**. As expected, due to their hybridization state the largest separations are observed on the aromatic carbons for the three chiral entities, while sp^3 carbon atoms show no or rather small separations. Globally smaller values are obtained for the purely organic chiral deriva-

(20) Ernst, R. R.; Bodenhausen, A.; Wokaun, G. *Principles of Nuclear Magnetic Resonance in One and Two Dimensions*; Clarendon Press: Oxford, U.K., 1987.

(21) Canlet, C.; Merlet, D.; Lesot, P.; Meddour, A.; Loewenstein, A.; Courtieu, J. *Tetrahedron: Asymmetry* **2000**, *11*, 1911.

tive. This result suggests that the complexation of $Cr(CO)_3$ by the arene group could amplify the mechanisms of chiral recognition by the polypeptide. Actually, the (η^6-arene)chromium tricarbonyl group could be seen as an electrostatic bulky entity that increases the anisotropy of the molecular shape. In addition, the noncomplexed aromatic ring gives the largest separations for the three related derivatives. The differences of ^{13}C CSA obtained for the benzylic group in **4** and **5** and even **6** are rather difficult to explain. An accurate analysis of all of the data is not trivial and requires complex calculations of order parameters[14] that are beyond the scope of this work, but general tendencies can be described. In the three compounds, chiral separations measured for the benzylic groups are rather large compared to values generally measured for simpler aromatic chiral compounds (generally below 25 Hz). This behavior is surprising because the ring is separated from the stereogenic center (C^7) by three bonds, and so small enantiodiscriminations could be expected for carbon atoms of this ring.

Due to the complexity of the chiral discrimination phenomenon in chiral ordered systems and because each molecule studied can be seen as a particular case, we have no definitive and absolute conclusion about this finding. Reasonnably, we can assume that related to both the molecular topology and the electronic properties (described by the van der Waals surface) of compounds **4**−**6**, the solute−PBLG interactions serve to orient the benzylic fragments for the *R* and *S* isomers very differently on average. As short-range interactions would be at the origin of the enantiomeric discrimination, this result could suggest that benzylic group is located rather close to the PBLG helices and would strongly experience the action of the enantiodiscrimination forces.

For a better understanding of the behavior of these compounds in PBLG phases, and in particular the origin of the strong increase of line widths for some carbon peaks in compounds **4** and **6**, we have recorded them in a PBLG/DMF-d_7 mixture. Note that such lyotropic mixtures also provide enantiodiscriminating oriented phases.[12,18] Sample compositions (samples 6 and 10) are listed in Table 3. Because a mixture of isotropic and anisotropic phases was obtained phase using DMF and PBLG with DP equal to 462, we prepared samples with higher DP (782). In both cases, variations of ^{13}C chemical shifts were observed compared with PBLG/chloroform due to the polarity of the co-organic solvent but the ^{13}C spectra can be easily analyzed.

In contrast to ^{13}C spectra in PBLG/chloroform, rather sharp peaks with an average line width of around 5 Hz are observed in PBLG/DMF solvent. From an enantiodiscrimination point of view, the results are contrasted. Here again spectral enantiodiscriminations are observed, but the situation is less favorable than in the PBLG/chloroform matrix because the number of discriminated sites and the magnitude of separations are significantly smaller (see Table 1). This result has been confirmed by adding small amounts of DMF in a PBLG/chloroform sample. Indeed, the successive additions of this polar cosolvent reduce both the chiral discrimination and the line width of peaks. This unexpected evolution is of interest. Indeed, it suggests that compounds **4** and **6** in the PBLG/DMF mixture are located on average farther than in PBLG/chloroform. In this case, enantiodiscrimination forces would act more weakly and, hence, smaller discriminations would be expected. In contrast, far from the PBLG helices the overall molecular tumbling of solute would be amplified (weak interactions with PBLG producing a very small ordering), thus increasing the T_2 relaxation times and so globally decreasing the line width.

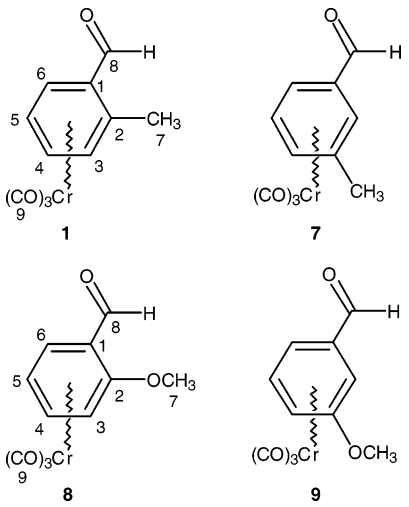

Figure 3. Molecular structures of the planar chiral aldehyde complexes studied (**1**, **7**, **8**, and **9**) and the numbering chosen for a simple comparison of spectral data.

There is no doubt that this result merits further studies using other examples. It highlights the role of surrounding solvent in the recognition mechanisms, but it also illustrates the current difficulty in predicting the magnitude of enantiodiscriminations, due to the important number of key parameters involved (temperature, polarity of cosolvent, nature and molecular shape of solute, ...), as well as the subtle balance of each parameter influencing the chiral discrimination mechanisms.

Analysis of Precursor Chiral Chromium Complexes. The synthesis of enantiopure chiral complexes such as **(*pR,S*)-4** requires the use of enantiopure precursor chiral chromium complexes such as the aldehyde **(*pR*)-1**. As evidence, the control of enantiomeric purity of these chiral organometallic starting materials is crucial.

To explore the potential of ^{13}C NMR in PBLG/chloroform, we have investigated a small collection of chiral chromium tricarbonyl complexes, with various substituents (methyl or methoxy) at two positions (ortho or meta substitution relative to the aldehyde function) on the η^6-arene group, as shown in Figure 3. In these series we have tried to analyze the influence of the electronegativity and the substitution pattern on the chiral discrimination. As illustration, Figures 4 and 5 show the $^{13}C\{^1H\}$ NMR spectrum of ***rac*-1** and ***rac*-7** recorded both in chloroform and in the PBLG mesophase, respectively. On the anisotropic ^{13}C spectrum we clearly show the variations of chemical shifts in comparison with those of the isotropic phase. In both cases, the shift of resonances is particularly important for the C^1 and C^4 aromatic atoms.

Disregarding solvent effects due to the polarity of the polymer, these shifts originate from a significant con-

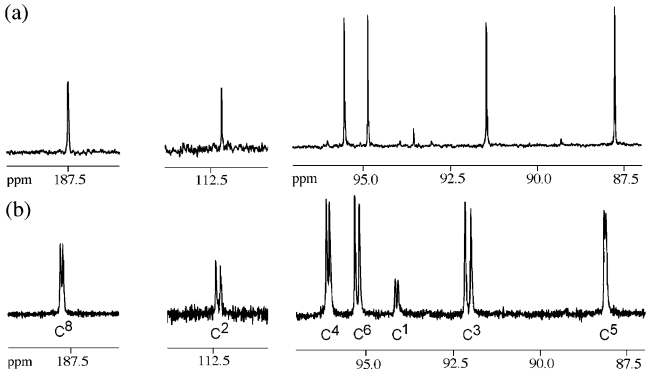

Figure 4. Part of the deshielded region of the 100 MHz $^{13}C\{^1H\}$ NMR spectrum of ***rac*-1** dissolved in (a) chloroform and (b) PBLG/chloroform. Both spectra were recorded with 4000 scans. Exponential (LB = 1 Hz) and Gaussian filtering (LB = −2 Hz, GB = 70%) were applied, respectively.

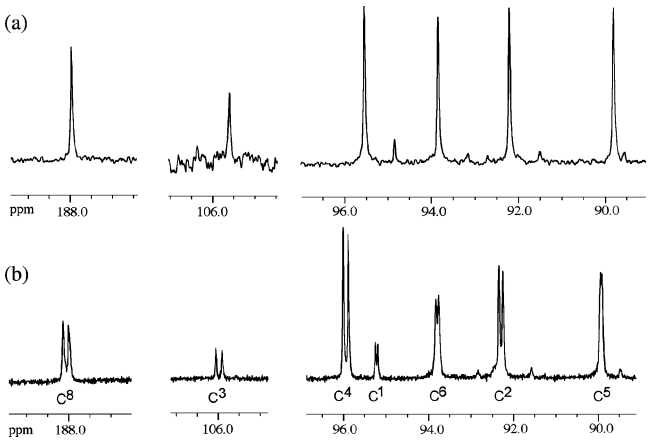

Figure 5. Part of the deshielded region of the 100 MHz $^{13}C\{^1H\}$ NMR spectrum of ***rac*-7** dissolved in (a) chloroform and (b) PBLG/chloroform using the same experimental data as for ***rac*-1**.

tribution of the anisotropic term $\Delta\sigma_C$ to ^{13}C chemical shifts measured in the oriented phase (see eq 2) related to the electron-withdrawing effects associated with the aldehydic substituent. Indeed, electron-withdrawing or donor electronic effects associated with a given substituent distort more or less the electronic cloud of aromatic carbons, depending on their positions in the ring (ipso > ortho > para > meta to the related substituent), and so tend to increase the electronic density anisotropy (in comparison with carbon atoms of benzene).

As previously, the comparison with the isotropic $^{13}C\{^1H\}$ spectrum indicates that various carbon atoms show spectral enantiodiscriminations on the ^{13}C CSA basis with differences varying between 4 and 17 Hz in both compounds. The differences measured for all sites are listed in Table 2. In these first two compounds, the position of the methyl group does not affect the magnitude of the discriminations.

To extend these results, we have investigated the case where the methyl group is replaced by a methoxy group in ortho and meta positions relative to the aldehyde group (compounds **8** and **9**). Here again enantiodiscriminations occur (see Table 2), but the magnitude of the spectral separations for compound **8** strongly differs from that of **9**, as well as from that of compounds **1** and **7**. Actually these results can be understood using mainly

Table 2. Differences of ^{13}C Chemical Shift (in Hz) for Chiral Compounds 1 and 7−9 in the PBLG/Chloroform Mesophase

		compound			
atom[a]	type of carbon	**1**	**7**	**8**	**9**
1	C/sp^2	8	5	25	7
2	C or CH/sp^2 [c]	14	9	31	0
3	C or CH/sp^2 [c]	17	16	35	<lw[b]
4	CH/sp^2	10	12	26	0
5	CH/sp^2	5	<lw[b]	28	9
6	CH/sp^2	13	7	37	<lw[b]
7	CH_3/sp^3	0	4	12	5
8	C/sp^2	7	14	31	11
9	C/sp^2	0	<lw[b]	7	0

[a] The numbering of carbon atoms is given in Figure 3. [b] Limit of enantioseparations: differences are below the line width of peaks. [c] Depending on the subtitution pattern.

electronic arguments. Indeed, for a given difference of orientational ordering between R and S (same carbon site), we can roughly expect better spectral enantiodiscriminations when the value of the tensor elements is large (eq 3). As mentioned above, the electronic properties of substituents have important effects on the $\Delta\sigma_C{}^{S \text{ or } R}$ value. Thus, for compounds **1** and **7**, the donor effect of the methyl (+I) group is weak compared to the electron-withdrawing effect of the aldehyde group (−M). Consequently, the electron-withdrawing effect governs mainly the electronic shape anisotropy of carbon atoms. In contrast, for compounds **8** and **9**, the donor effect of the methoxy group (+M) is much stronger than that of the methyl group, and so the position of this group relative to the aldehyde can generate different electronic situations for each aromatic carbon atom. Thus, synergistic electronic effects occur for the ortho-disubstituted η^6-arene species **8**, leading to amplify the anisotropy of electronic density shape for all aromatic carbon sites. In contrast, antagonistic electronic effects arise for the meta-disubstituted η^6-arene species **9** because the donor effect balances more or less the electron-withdrawing effect, and so the shape anisotropy of the electron cloud is smaller. Under these conditions we can expect, for a given differential ordering, a lower spectral separation for **9** compared with that for compound **8**.

Proton-Coupled Carbon-13 2D NMR. As can be seen in Table 2, rather small chiral discrimination was observed for the carbon atom of the methyl group C^7 on the basis of differences of ^{13}C CSA (see Table 2). Under these circumstances, it may be pertinent to record the proton-coupled carbon-13 1D spectrum in order to detect the separation of enantiomers through a difference in the proton−carbon-13 residual dipolar couplings, D_{CH}. This interaction can be written as[17,18]

$$D_{C-H}{}^{S \text{ or } R} = -\frac{h\gamma_{13C}\gamma_{1H}}{4\pi^2}\left\langle \frac{S_{C-H}{}^{S \text{ or } R}}{r_{C-H}{}^3} \right\rangle \qquad (4)$$

with

$$S_{C-H}{}^{S \text{ or } R} = \sum_{\alpha,\beta = a,b,c} \cos\theta_\alpha{}^{C-H} \times \cos\theta_\beta{}^{C-H} \times S_{\alpha\beta}{}^{S \text{ or } R} \qquad (5)$$

where $\theta_\alpha{}^{C-H}$ and $\theta_\beta{}^{C-H}$ are the angles between the axes of the molecular frame (a, b, c) and the internuclear C−H bond. The brackets denote an ensemble average

Table 3. Composition of Liquid Crystalline NMR Samples Investigated

sample	solute	polymeric solvent	DP[a] PBLG/PBDG	cosolvent	solute, mg[b]	polymer, mg[b]	cosolvent, mg[b]	polymer wt, %
1	***rac*-1**	PBLG	463	$CHCl_3$	58	140	399	23.4
2	**(*pS*)-1**	PBLG	463	$CHCl_3$	25	140	427	23.4
3	***rac*-4**	PBLG	463	$CHCl_3/CDCl_3$	15	140	75/326	25.1
4	***rac*-4**	PBG	463/914	$CHCl_3/CDCl_3$	15	69/71	74/325	25.1
5	**(*pR,S*)-4**	PBLG	463	$CHCl_3/CDCl_3$	16	141	76/321	25.4
6	***rac*-4**[c]	PBLG	782	DMF-d_7	6	130	310	29.1
7	***rac*-5**	PBLG	463	$CHCl_3/CDCl_3$	15	142	75/325	25.4
8	***rac*-6**	PBLG	463	$CHCl_3/CDCl_3$	7	140	74/326	25.6
9	***rac*-6**	PBG	463/914	$CHCl_3/CDCl_3$	7	73/67	75/325	25.6
10	***rac*-6**[c]	PBLG	782	DMF-d_7	7	131	312	29.1
11	***rac*-7**	PBLG	463	$CHCl_3$	61	139	400	23.2
12	***rac*-8**	PBLG	463	$CHCl_3$	60	139	402	23.1
13	***rac*-9**	PBLG	463	$CHCl_3$	59	140	401	23.3

[a] DP = degree of polymerization of polypeptide (PBLG and PBDG) used. [b] The accuracy in the weighing is 1 mg. [c] Note that, in the case of DMF, it is necessary to heat the mixture in order to dissolve the polymer easily during the sample preparation.

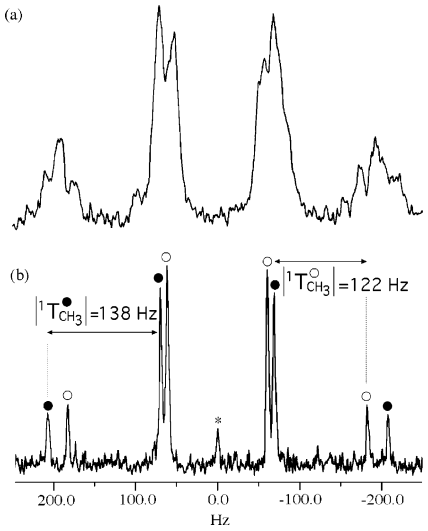

Figure 6. Signal of the methyl group of (***rac*)-7** extracted from the ^{1}H-coupled ^{13}C spectrum (a) and ^{13}C$-^1$H HETSERF 2D map (b). The 1D spectrum was recorded with 2000 scans. In both cases, a Lorentzian filtering was applied ($LB_{1,2}$ = 2 Hz). The small peak at 0 Hz is an artifact.

on intramolecular motions. In practice, separations observed between resonances in ^{13}C$-^1$H spectral patterns are equal to the total ^{13}C$-^1$H coupling, denoted T_{CH}, that is equal for a ^{13}C$-^1$H interacting internuclear pair separated by one bond:

$$|^1T_{CH}| = |^1J_{CH} + 2^1D_{CH}| \quad (6)$$

To illustrate this fact, Figure 6a presents an expansion of the proton-coupled carbon-13 spectrum of ***rac*-7** centered on the methyl group signal. Unfortunately, in this example the signal shows a complex unresolved spectral pattern that cannot be interpreted easily. Consequently, it is not possible to unambiguously claim that enantiomers are differentiated here. This kind of unresolved structure is generally observed when long-range proton−carbon dipolar couplings (here with the aromatic protons) are numerous. To overcome this situation, some of us have recently shown the practical efficiency of heteronuclear selective *JD*-resolved 2D experiments, denoted as HETSERF.[22] This experiment, derived from the well-known *J*-resolved experiment, permits the extraction of ^{1}H$-^{13}$C residual dipolar couplings for each enantiomer by exciting a single type of proton. After a double Fourier transform, the resulting 2D map shows the spectral pattern associated with the selected ^{1}H$-^{13}$C pairs in the F_1 dimension, while the proton-decoupled ^{13}C spectrum appears in the F_2 dimension. Figure 6b displays the ^{13}C signal of the methyl group of ***rac*-7** extracted from the ^{13}C$-^1$H HETSERF 2D map obtained by selective excitation of three equivalent methyl protons. Here we observe two distinct quartets centered on the same chemical shift (no differences of ^{13}C CSA): one for each enantiomer. In this example, $|^1T_{CH}|$ is equal to 122 and 138 Hz, corresponding to a value for $^1D_{CH}$ equal fortuitously to 4 and −4 Hz. Through this example, we demonstrate that ^{1}H$-^{13}$C selective refocusing 2D experiments provide a valuable NMR tool for analyzing enantiomer mixtures.

Conclusion

In this work we have explored the analytical potential of proton-decoupled ^{13}C 1D NMR and proton-coupled ^{13}C 2D NMR in weakly orienting solvents for studying planar chiral (η^6-arene)chromium tricarbonyl complexes. As the main result, we have shown that PBLG mesophases are sufficiently stable in the presence of chromium species to record ^{13}C spectra and are able to interact differently with enantiomers of this class of chiral compounds. Also we demonstrated here that this technique provides an interesting alternative to existing classical methods without any chemical modifications of the investigated chiral compounds. In addition, taking advantage of modern NMR spectrometers operating with higher magnetic field, we could improve both the sensitivity of the method and the magnitude of spectral enantiodiscriminations observed in these examples. Thus, operating at 18.8 T (200 MHz for ^{13}C NMR), we should observe particularly large spectral enantiodiscriminations based on ^{13}C CSA differences. For instance, the C^{12} carbon atom in compound **5** should a priori show enantioseparation at about 320 Hz. There is no doubt that successful results would be also obtained using deuterium NMR if the various compounds investigated here were deuterated. In this case, spectral enantiodiscriminations would be observed on the basis of quadrupolar splitting differences.[10,12] Among analytical applications of this approach, we have validated the ee value

(22) Farjon, J.; Baltaze, J. P.; Lesot, P.; Merlet, D.; Courtieu, J. *J. Magn. Reson. Chem.* **2004**, *42*, 594.

of β-amino alcohol derivatives obtained by a new asymmetric cross-coupling reaction.

Experimental Section

Preparation and Analysis of the (η^6-arene)Cr(CO)$_3$ Complexes and Ligand 6. The β-*N*-hydroxylamino alcohols ***rac*-4**, (***pR,S*)-4**, ***rac*-5**, and ***rac*-6** were prepared according to the procedure we described in ref 6. The ^{13}C signal of $CDCl_3$ is used as internal reference at 77.0 ppm.

***rac*-4.** ^{1}H NMR ($CDCl_3$, 400 MHz): δ (ppm) 7.48−7.34 (m, 5H, H$^{13-17}$), 6.38 (d, 1H, J = 6.6 Hz, H^6), 5.64 (t_{app}, 1H, J = 6.2 Hz, H^4), 5.05 (t_{app}, 1H, J = 6.1 Hz, H^5), 4.96 (d, 1H, J = 6.6 Hz, H^3), 4.79 (broad d, 2H, J = 13.1 Hz, H^{11}, OH), 3.97 (d, 1H, J = 12.9 Hz, H$^{11'}$), 3.62 (broad s, 1H, OH), 3.52 (s, 1H, H^7), 2.16 (s, 3H, H^{18}), 1.31 (s, 3H, H^9 or H^{10}), 1.14 (s, 3H, H^9 or H^{10}). ^{13}C NMR ($CDCl_3$, 100 MHz): δ (ppm) 233.5 (C^{19}), 137.2 (C^{12}), 129.6 (C^{13,17}), 128.6 (C^{14,16}), 127.8 (C^{15}), 111.2 (C^2), 104.4 (C^1), 100.0 (C^6), 97.4 (C^4), 90.5 (C^3), 86.4 (C^5), 75.2 (C^8), 68.7 (C^7), 62.9 (C^{11}), 28.7 (C^9 or C^{10}), 26.7 (C^9 or C^{10}), 21.1 (C^{18}). EI-MS: *m/z* 337 ([M] − 3[CO]). IR (ATR): ν_{CO} (cm^{-1}) 1955, 1863.

(*pR,S*)-4. $[\alpha]_D^{20}$ = +150° (c = 0.26; $CHCl_3$).

***rac*-5.** ^{1}H NMR ($CDCl_3$, 200 MHz): δ (ppm) 7.39−7.30 (m, 5H, H$^{13-17}$), 6.38 (d, 1H, J = 6.5 Hz, H^2 or H^6), 5.61 (t_{app}, 1H, J = 6.1 Hz, H^4), 5.49 (d, 1H, J = 6.5 Hz, H^6 or H^2), 5.31 (broad s, 1H, OH), 5.20−5.08 (m, 2H, H^{3,5}), 4.59 (d, 1H, J = 13.0 Hz, H^{11}), 3.95 (d, 1H, J = 13.0 Hz, H$^{11'}$), 3.74 (broad s, 1H, OH), 3.25 (s, 1H, H^7), 1.32 (s, 3H, H^9 or H^{10}), 1.23 (s, 3H, H^9 or H^{10}). ^{13}C NMR ($CDCl_3$, 100 MHz): δ (ppm) 233.0 (C^{19}), 137.5 (C^{12}), 129.5 (C^{13,17}), 128.6 (C^{14,16}), 127.7 (C^{15}), 104.6 (C^1), 98.5 (C^6 or C^2), 98.3 (C^2 or C^6), 96.2 (C^4), 88.7 (C^3 or C^5), 88.1 (C^5 or C^3), 74.9 (C^7), 74.4 (C^8), 63.0 (C^{11}), 29.3 (C^9 or C^{10}), 27.4 (C^9 or C^{10}). EI-MS: *m/z* 323 ([M] − 3[CO]). IR (ATR): ν_{CO} (cm^{-1}) 1957, 1862.

***rac*-6.** ^{1}H NMR ($CDCl_3$, 400 MHz): δ (ppm) 7.64 (d, 1H, J = 7.4, H^6) 7.28−7.18 (m, 9H, H^{arom}), 5.03 (broad s, 1H, OH), 4.55 (broad s, 1H, OH), 4.20 (s, 1H, C^7), 3.75 (d, 1H, J = 13.4 Hz, H^{11}), 3.48 (d, 1H, J = 13.4 Hz, H$^{11'}$), 2.41 (s, 3H, CH_3), 1.40 (s, 3H, H^9 or H^{10}), 1.03 (s, 3H, H^9 or H^{10}). ^{13}C NMR ($CDCl_3$, 100 MHz): δ (ppm) 137.9 (C^{12}), 137.1 (C^2 or C^1), 137.0 (C^1 or C^2), 130.7 (C^3), 129.2 (C^{13,17}), 128.3 (C^{14,16}), 128.1 (C^6), 127.3 (C^5+C^{15}), 126.0 (C^4), 75.0 (C^8), 73.5 (C^7), 62.8 (C^{11}), 27.9 (C^9 or C^{10}), 25.0 (C^9 or C^{10}), 21.0 (C^{18}).

Preparation and Analysis of the (aldehyde η^6-arene)-Cr(CO)$_3$ Complexes. The (η^6-benzaldehyde)Cr(CO)$_3$ derivatives ***rac*-1**,[23,24] ***rac*-7**,[24] ***rac*-8**,[24] and ***rac*-9**[24] were synthesized either by oxidation of the corresponding benzylic alcohols complexes[23] or by complexation of the corresponding acetals.[25]

The enantiopure aldehyde **(*pR*)-1** was prepared by resolution of ***rac*-1**, as described in ref 3.

(*pR*)-1. $[\alpha]_D^{20}$ = +650° (c = 0.22; $CHCl_3$).

***rac*-1.** ^{1}H NMR ($CDCl_3$, 200 MHz): 9.79 (s, 1H, H^8), 6.05 (d, 1H, J = 6.6 Hz, H^6), 5.71 (t_{app}, 1H, J = 6.3 Hz, H^4), 5.21 (t_{app}, 1H, J = 6.3 Hz, H^5), 5.02 (d, 1H, J = 6.2 Hz, H^3), 2.51 (s, 3H, H^7). ^{13}C NMR ($CDCl_3$, 100 MHz): 230.4 (C^9); 187.5 (C^8), 111.8 (C^2), 95.5 (C^4), 94.8 (C^6); 93.5 (C^1), 91.4 (C^3), 87.7 (C^5), 18.2 (C^7).

***rac*-7.** ^{1}H NMR ($CDCl_3$, 200 MHz): 9.49 (s, 1H, H^8), 5.78 (s, 1H, H^2), 5.77 (d, 1H, J = 6.3 Hz, H^6), 5.56 (d, 1H, J = 6.3 Hz, H^4), 5.36 (t_{app}, 1H, J = 6.3 Hz, H^5), 2.25 (s, 3H, H^7). ^{13}C NMR ($CDCl_3$, 100 MHz): 230.9 (C^9), 188.4 (C^8), 106.0 (C^3), 96.0 (C^4), 95.3 (C^1), 94.3 (C^6), 92.6 (C^2), 90.2 (C^5), 20.5 (C^7).

***rac*-8.** ^{1}H NMR ($CDCl_3$, 400 MHz): 10.02 (s, 1H, H^8), 6.21 (d, 1H, J = 6.1 Hz, H^6), 5.84 (t_{app}, 1H, J = 5.8 Hz, H^4), 5.05 (d, 1H, J = 6.6 Hz, H^3), 4.98 (t_{app}, 1H, J = 5.8 Hz, H^5), 3.84 (s, 3H, H^7). ^{13}C NMR ($CDCl_3$, 100 MHz): 230.5 (C^9), 185.4 (C^8), 145.7 (C^2), 94.8 (C^4), 92.4 (C^6), 86.2 (C^1), 84.3 (C^5), 72.1 (C^3), 56.0 (C^7).

***rac*-9.** ^{1}H NMR ($CDCl_3$, 400 MHz): 9.57 (s, 1H, H^8), 5.56 (s, 1H, H^2), 5.54 (t_{app}, 1H, J = 6.6 Hz, H^5), 5.47 (d, 1H, J = 6.6 Hz, H^6), 5.43 (d, 1H, J = 6.1 Hz, H^4), 3.72 (s, 3H, H^7). ^{13}C NMR ($CDCl_3$, 100 MHz): 231.1 (C^9), 189.5 (C^8), 140.7 (C^3), 95.9 (C^1), 97.9 (CDCl